Seasonality patterns in global vegetation burning

José M.C. Pereira[1], Akli Benali[1], Duarte Oom[1] Bernardo Mota[1], and Yannick Le Page[2]

[1]Centro de Estudos Florestais, Instituto Superior de Agronomia,
Universidade Técnica de Lisboa
Tapada da Ajuda, 1349-017 Lisboa Portugal
jmocpereira@gmail.com, aklibenali@gmail.com, duarte.oom@gmail.com, bmota@isa.utl.pt

[2]Global Ecology Lab, Department of Geographical Sciences, University of Maryland
2181 Samuel J. LeFrak Hall, College Park, MD 20742, USA
yannick.lepage@pnnl.gov

Abstract. Vegetation fires display marked seasonality, which is controlled by a combination of climatic factors and land use management practices, has not been thoroughly characterized at the global scale. We used active fire counts from the Moderate Resolution Imaging Spectrometer (MODIS), aggregated at 0.5º spatial resolution, over the period 2001-2009, to derive maps of fire season start, peak, end, and duration. This analysis relied on TIMESAT, a software package originally developed to extract seasonal parameters from time series of satellite imagery. Active fire count time series were fitted with a Savitsky-Golay filter, and seasonality parameters were extracted from the fitted functions. We also developed the first ever global analysis of fire season modality, classifying global fire activity into uni- and bimodal fire seasons. This classification relied on the use of circular statistics techniques, namely fitting a single von Mises distribution, or a mixture of two distributions. Model fit was assess with the Nash-Sutcliff model efficiency index. The largest concentration of cells with bimodal fire season was found in the Ukraine, Kazakhstan, and southern Russia. Areas with complex fire seasonality, and which were left unclassified pending methodological refinement, are located in the southeastern USA, southern South America, southeastern China and southeastern Australia.

1. Introduction.

The occurrence of vegetation fires is characterized by a strong annual cycle. The fundamental aspect of this cycle is the alternation of a fire-free season and a fire occurrence season, which is mostly controlled by climate (Dwyer et al., 2000; Giglio et al., 2006). On intra-seasonal time-scales, the distribution of fire activity depends on the dynamics of the factors controlling fire ignition, fire spread and fire extinction. Fine vegetation or dead fuels lose moisture rapidly after the dry season starts, becoming prone to early season fires, especially in grasslands and savannas. Live and woody vegetation has slower moisture dynamics, and fire susceptibility may be reached only late in the dry season, as in tropical forests (Le Page et al., 2010).

Land use management practices also influence fire seasonality. Agricultural burning is used world-wide for soil fertilization (pre-seeding fires), to prepare fields for harvest work (e.g. sugar cane pre-harvest fires) and to dispose of crop residues (post-harvest fires) (Yevich & Logan, 2003; Korontzi et al., 2006). At large-scale tropical forest conversion sites (Morton et al., 2008) and in most shifting cultivation systems (Thrupp et al., 1997), the area to be deforested is cut at the end of the wet season, and fires are set repeatedly late in the dry season to maximize fuel consumption. In this overview of seasonality of global vegetation burning, we briefly review previous research, emphasizing the study of time lags between

meteorological fire weather severity and actual fire occurrence of Le Page et al. (2010). We also present new results on global fire seasonality quantification and on the classification of fire regimes with unimodal an bimodal seasonality.

2. Methods

2.1. Global fire season timing

TIMESAT (Jönsson & Eklundh, 2004) was used to estimate the start, peak, and end dates of the fire season, using MODIS active fire counts at 0.5ºspatial resolution, for the priod 2001-2009. TIMESAT was developed to extract seasonal parameters from normalized difference vegetation index (NDVI) time series and can process data of any temporal resolution. It offers different least-squares methods for processing time-series of remotely sensed data. The first method uses local polynomial functions as an adaptive Savitzky–Golay filter. The other two are least-squares methods that fit data using double logistic and asymmetric Gaussian functions, respectively (Heumann et al., 2007). A pre-filtering step removes outliers within a single time series and eliminates time series with unclear seasonality. Next, an adaptation step generates smooth time series of the pre-filtered data. Finally, a set of seasonal parameters is extracted (Fig. 1). Le Page et al. (2010) adapted TIMESAT to process interrupted time series, such as those of fire activity, which ceases during the local rainy season. Further, we carefully selected the user adjustable processing parameters. Pre-filtering rules were defined, to test for plausible fire activity and seasonality patterns. In the adaptation step, we used the Savitzky–Golay three-step adaptive filtering. Standard TIMESAT seasonal parameters were then extracted, including start, peak, and end of the fire season. The start data was defined as the date when the cumulative fire counts reach 5% of the total annual counts, and the end date at 95% cumulative fire counts. Peak fire date corresponds the maximum value, in fire counts, of the fitted function.

2.2 Unimodal vs. bimodal fire regime classification

The fire season was defined on a 0.5º grid cell and 16-day composites, using MODIS global monthly active fire location product (MCD14ML, collection 5) for the period 2001-2011. The data were previously screened using the approach of Mota et al. (2006) and Oom and Pereira (2012). The normalized active fire counts for each year (counts in each 16-day composite / annual total) detected in each grid cell and time composite over the study period were plotted as a circular histogram and fitted with a mixture of *N* von Mises probability distributions (Fisher, 1995). For any given grid cells, years with fewer than six fire counts were excluded from further analysis. The number of von Mises distributions used varied from 1 to 2 corresponding, to uni and bimodal distributions, respectively. For each component (j) the probability density function is defined by Eq. 1:

$$vM_j(\theta;\kappa_j;\mu_j) = \frac{1}{2\pi I_0(\kappa_j)}\exp[\kappa_j \cos(\theta-\mu_j)] \ , \quad 0 \le \theta < 2\pi \qquad (1)$$

where, $\kappa_j \geq 0$ and $0 \leq \mu_j < 2\pi$ are the concentration and mean parameters, respectively. The probability model of the mixture of von Mises distributions mvM(Θ) is given by Eq. 2:

$$mvM(\theta) = \sum_{j=1}^{N} \omega_j vM_j(\theta) \quad (2)$$

where, $0.05 \leq \omega_j \leq 0.95$ is the mixture proportion of each component and $\sum_{j=1}^{N} \omega_j = 1$

The mixture model was optimised by estimating its parameters to obtain the best fit between observed and predicted normalized active fire cumulative frequency. The single independent variable was day of the year (recoded in radians). The non-linear optimisation performed with automatic Newton search method, minimizing the square of absolute differences between observations and estimates. The only constraint applied to the parameter search space was $\kappa_j \geq 0.1$, to avoid fitting uniform distributions (Fisher, 1995), which do not exhibit significant fire seasonality.

Model performance was evaluated with the Nash–Sutcliffe model efficiency index (hereafter, MEF), a measure of model predictive power (Nash and Sutcliffe, 1970). The index was calculated considering the observed and estimated normalised, non-cumulative, fire frequencies. For each pixel, the circular mixture model with the highest MEF was selected, regardless of the number of parameters involved, guaranteeing the best possible fit. Cells with MEF < 0.7 were considered poor fits to the data, and were not classified. The fire seasonality at a given cell was considered bimodal if MEF for the mixture of two von Mises distributions was at least 0.2 units higher than MEF for a single distribution, otherwise fire seasonality was considered unimodal. A cell with a bimodal fit is reclassified as unimodal if the temporal difference between the two modes is smaller than three months. An additional requirement for bimodality is that the secondary fire season must contain at least 5% of the total number of annual fire counts.

4. **Results**

The TIMESAT analysis of the MODIS active fire counts, aggregated at 0.5º spatial resolution, for the period 2001-2009, allowed for rigorous estimation of fire seasonality parameters. Figures 1 and 2 show, respectively, the two-month period during which peak fire activity is reached, and the length of the fire season at each cell. Most of the global land area was covered by the analysis. In the higher latitudes of the northern hemisphere, a clear latitudinal gradient is observed, with burning peaking in July-August in the northernmost regions, and gradually shifting towards peak dates earlier in the year. A latitudinal pattern is also visible in Africa, with a November-December peak in fire activity in northern hemisphere Africa and a broader (July-October) peak period in southern hemisphere Africa.

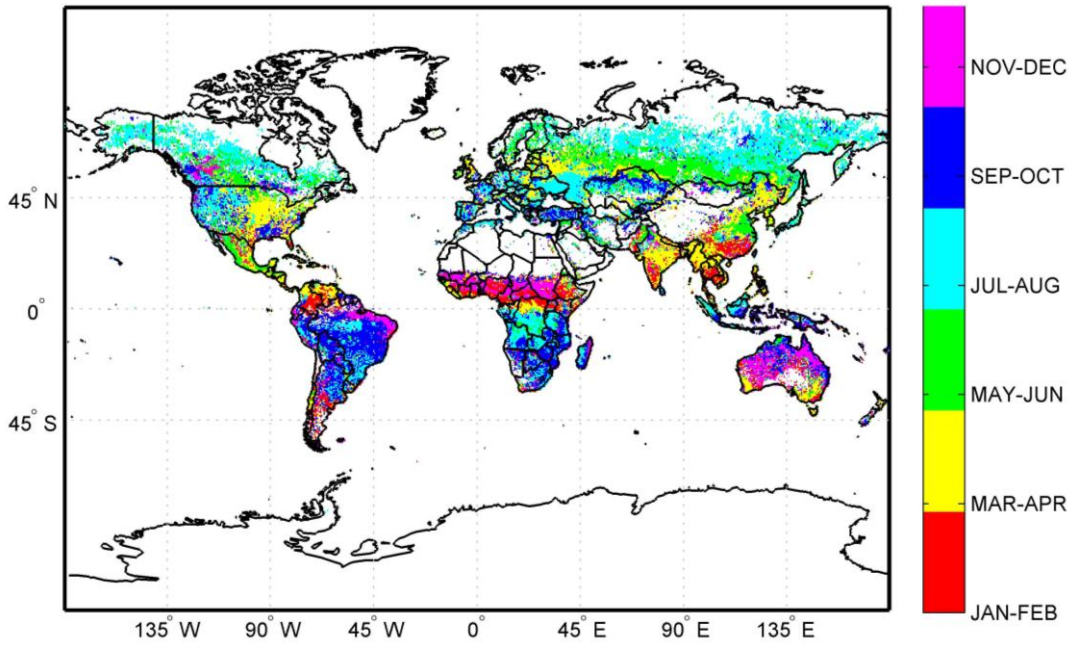


Figure 1. Fire season bi-monthly peak period.

Regarding fire duration, it is longer in tropical regions, and in scattered areas throughout the higher latitudes of the northern hemisphere, which show strong local contrast in length of the fire season.

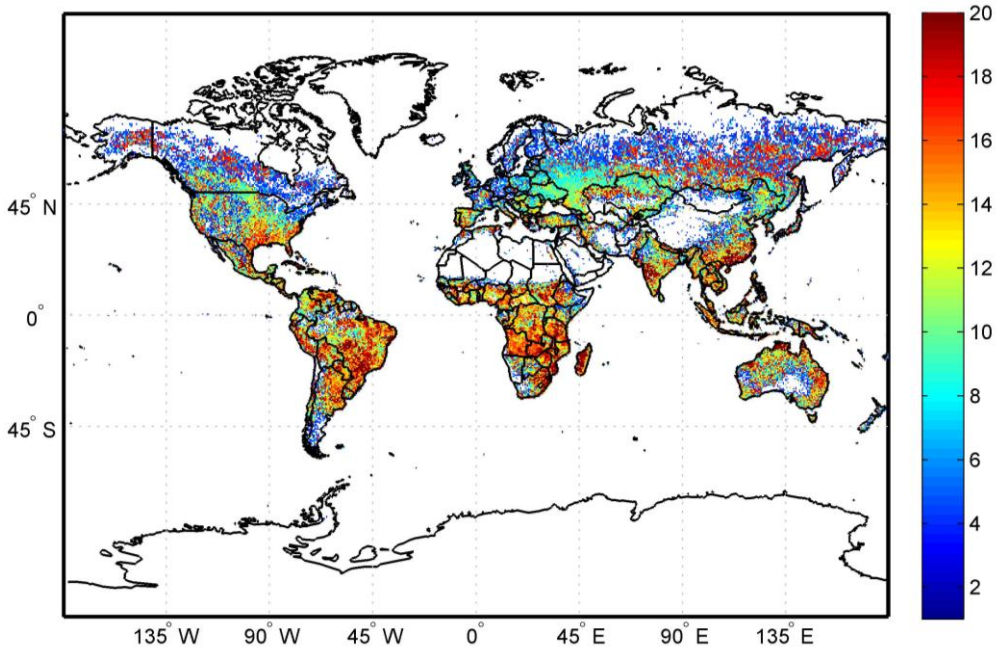


Figure 2. Fire season duration, in number of 10-day composite periods.

Analysis of fire regime modality with circular statistics using the von Mises distribution (Figure 3) resulted in a preliminary classification of global fire regimes, according to the uni- or bimodality of the fire season.

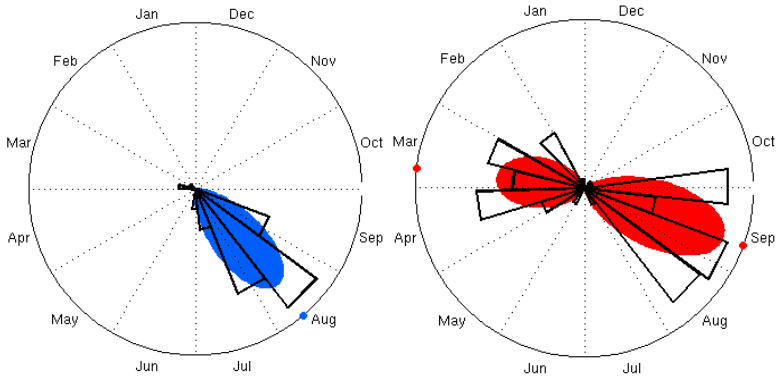


Figure 3. Examples of unimodal (left, blue) and bimodal (right, red) fire seasons, fitted with a single von Mises distribution (left) and a mixture of two von Mises distributions (right).

The circular statistics analysis, complemented with some additional criteria, produced the global classification shown in figure 4. Most global area displays unimodal fire seasons, with bimodal seasons concentrated in the predominantly agricultural areas of the Ukraine, Kazakhstan and southwestern Russia, parts of the north American Midwest, the Indus river headwaters, some areas in SE Australia. Large areas of more complex fire seasonality patterns (not assigned, grey) can be seen in these USA, SE China, southern S. America, and SE Australia.

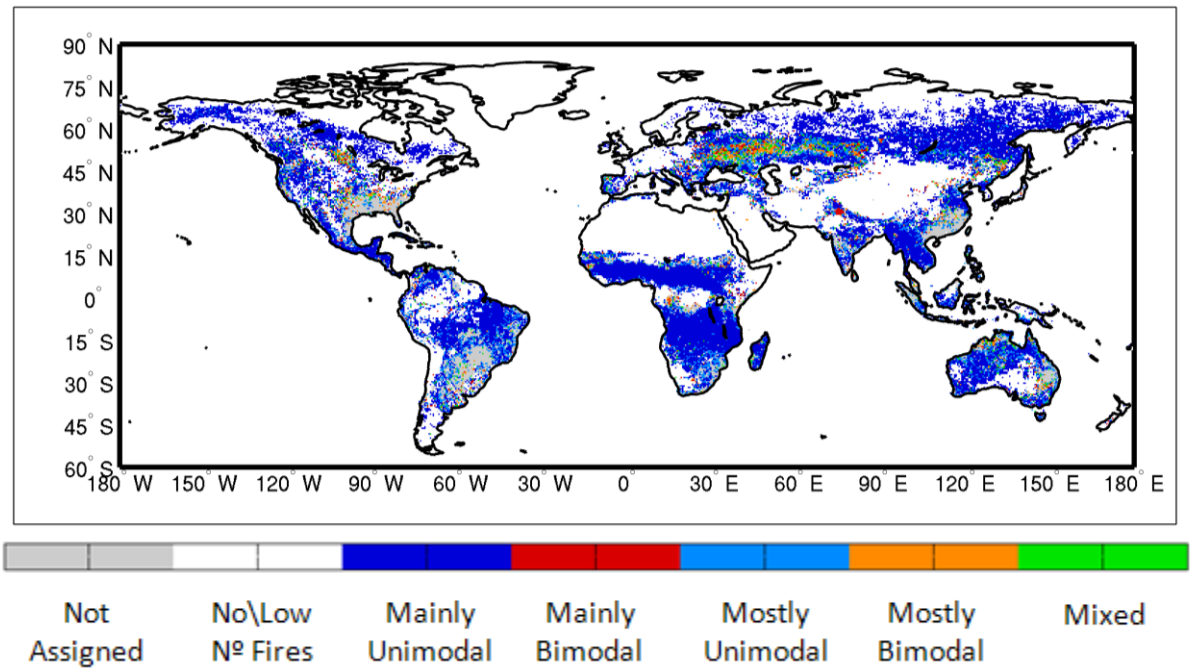


Figure 4. Global classification of fire regime modality.

4. Conclusions.

Analysis of spatially aggregated daily MODIS active fire data, assisted by quantitative techniques of time series filtering and circular statistics techniques allowed for rigorous, quantitative estimation of fire seasonality parameters, namely start, peak, and end dates, as well as season duration. Additionally, and for the first time, a global classification of fire seasonality is presented, which should be considered preliminary. Nevertheless, it shows that bimodal fire seasons occupy a significant fraction of the fire-prone land surface, a pattern that deserves further exploration and interpretation.

5. References.

Dwyer, E., Pereira, J.M.C., Grégoire, J.M. & Dacamara, C.C. (2000) Characterization of the spatio-temporal patterns of April 1992 to March 1993. **Journal of Biogeography**, 27, 57–69.

Fisher, N.I. (1995) **Statistical Analysis of Circular Data**. Cambridge University Press, 296 pp.

Giglio, L., Csiszar, I. & Justice, C.O. (2006a) Global distribution and seasonality of active fires as observed with the Terra and Aqua Moderate Resolution Imaging Spectroradiometer (MODIS) sensors**. Journal of Geophysical Research-Biogeosciences**, 111, G02016.

Heumann, B.W., J.W. Seaquist, L. Eklundh, P. Jönsson (2007) AVHRR derived phonological change in the Sahel and Soudan, Africa, 1982–2005. **Remote Sensing of Environment**, 108, (4): 385–392. http://dx.doi.org/10.1016/j.rse.2006.11.025.

Jönsson, P. & Eklundh, L. (2004) TIMESAT – a program for analyzing time-series of satellite sensor data. Computers and Geosciences, 30, 833–845.

Korontzi, S., McCarty, J., Loboda, T., Kumar, S. & Justice, C. (2006) Global distribution of agricultural fires in croplands from 3 years of Moderate Resolution Imaging Spectroradiometer (MODIS) data. **Global Biogeochemical Cycles**, 20, G–2021. doi:10.1029/2005GB002529

Le Page, Y., D. Oom, J.M.N. Silva, P. Jönsson and J.M.C. Pereira (2010) Seasonality of vegetation fires as modified by human action: observing the deviation from eco-climatic fire regimes. **Global Ecology and Biogeography**. 19 (4): 575-588. DOI: 10.1111/j.1466-8238.2010.00525.x

Mota, B., J.M.C. Pereira, D. Oom, M.J.P. Vasconcelos, and M. Schultz (2006). Screening the ESA ATSR-2 World Fire Atlas (1997-2002). **Atmospheric Chemistry and Physics**, 6: 1409-1424.

Nash, J. E. and J. V. Sutcliffe (1970), River flow forecasting through conceptual models part I - A discussion of principles. **Journal of Hydrology**, 10 (3), 282–290.

Oom, D., J.M.C. Pereira, Exploratory spatial data analysis of global MODIS active fire data, **International Journal of Applied Earth Observation and Geoinformation**, Available online 28 Sept. 2012, ISSN 0303-2434, 10.1016/j.jag.2012.07.018.

Thrupp, L.A., Hecht, S. & Browder, J. (1997) **The diversity and dynamics of shifting cultivation: myths, realities, and policy implications**. World Resources Institute, Washington, DC.

Yevich, R. & Logan, J.A. (2003) An assessment of biofuel use and burning of agricultural waste in the developing world. **Global Biogeochemical Cycles**, 17, 1095. doi:10.1029/2002GB001952.